Mixed SAMs of backbone-functionalized tribenzotriquinacenes and alkanethiols: Synthesis, preparation and STM-investigations

Stefan Henne, Björn Bredenkötter, Dirk Volkmer*

Institute of Physics, Chair of Solid State and Materials Chemistry, Augsburg University, Universitätsstrasse 1, D-86159 Augsburg, Germany

1. Introduction

In the field of nanotechnology, the design, construction and study of simple nano-sized molecular devices are topics of current interest [1]. The technological potential of such devices can only be fully exploited if the device, or at least one of its components is attached to a surface, which opens up the possibility for active manipulation or switching at nanoscale spatial resolution. Our particular approach toward anchored nanodevices includes rigid TBTQ molecular building blocks, serving as stator of nanomechanical devices, the rotor part being represented by C_{60} fullerene derivatives [2]. The tribenzotriquinacene motif is particularly suitable for this approach, because it is a rigid receptor molecule [3], which can be substituted at its peripheral positions (Scheme 1) to create a half-bowl shaped cavity, while at the same time a large variety of chemical groups can be introduced in its bridgehead positions (Scheme 1), serving as a means to attach TBTQ to different surfaces.

Initial studies were focused on TBTQ derivatives that form stable host–guest complexes with fullerene C_{60} in solution [4,5]. Subsequent investigations were targeted on the structural optimization of the peripheral positions of TBTQ receptors with the intention to increase [$C_{60} \subset$ TBTQ] complex stability [6], and thus to enable formation of a self-assembled mechanical nanodevice, including the potential to perform unidirectional rotation [7], a fundamental operation mode of almost any functional device.

Continuing this research line, we here address the critical question as to how [$C_{60} \subset$ TBTQ] complexes might be positioned on a (flat) surface. One possible solution for this challenge lies in the functionalization of the bridgehead positions of the TBTQ receptor, which was optimized with the purpose to embed them into structurally well-defined simple monolayers, deposited on Au-(1 1 1) surfaces [8]. Self-assembled organosulfur monolayers, which contain an alkyl chain with a surface-active sulfur group, such as thiols [9], di-*n*-alkyl disulfides [10] or di-*n*-alkyl sulfides [11] seem to be particularly suitable for embedding and integrating concave host molecules, which has been previously demonstrated for calixarenes [12], resorcarenes [13] and cyclotriveratrylenes [14].

The aim of the present study is to work out an appropriate surface-anchor-system for TBTQs. In present and future studies more detailed investigations are in progress or planned. These include, for example, the synthesis of a TBTQ which contains a cavity for the embedding of C_{60} and an anchor group, which is challenging because the known preparative routes for the modification peripheral and bridgehead position are not compatible to each other. Furthermore, it is unclear in which way the SAM will influence the kinetic and thermodynamic of the [$C_{60} \subset$ TBTQ] complex. Subsequently, the loading density of the TBTQ in the SAM and of C_{60} in the TBTQ has to be optimized.

In the studies, we are presenting here, di-*n*-alkyl sulfide functionalities are employed as surface-anchoring groups (Scheme 1), the interaction of which with the Au-(1 1 1)-surface is expected to be more reversible than that of thiols, thus facilitating a structurally

* Corresponding author.
E-mail address: dirk.volkmer@physik.uni-augsburg.de (D. Volkmer).

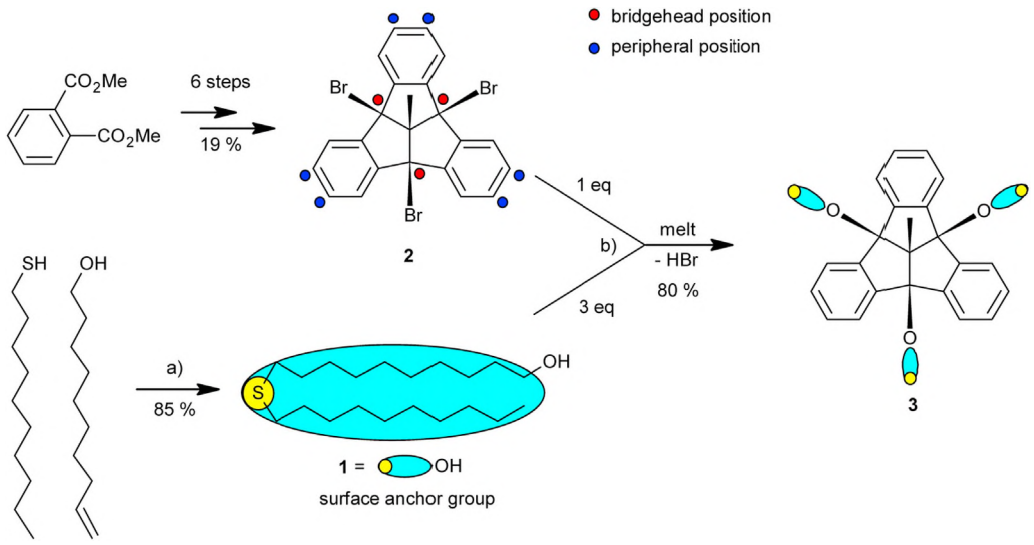

Scheme 1. Preparative route to TBTQ **3**. (a) 9-BBN, THF, 0 °C, 2 h; (b) 70 °C, 12 h.

well-defined integration of **3** in the supporting alkanethiol monolayers. In this way, every TBTQ **3** is attached to the Au-(1 1 1) surface via three di-*n*-alkyl sulfide anchor groups connected to the bridgehead positions of TBTQ, which accordingly exposes its central, fully accessible cavity to the mixed monolayer surface.

In the following, the synthesis of 4b,8b,12b-tris(10-(decylsulfanyl)decyloxy)-12d-methyl-4b,8b,12b,12d-tetrahydrodibenzo[2,3:4,5]pentaleno[1,6-*ab*]inden (TBTQ **3**), which contains three di-*n*-decylsulfide chains as anchor groups for Au-(1 1 1), is described for the first time. Thereafter, a method, for embedding isolated molecules of the minor component **3** into a closely packed matrix of alkanethiols on Au-(1 1 1) is described and the resulting mixed SAMs [15], are characterized by STM under ambient conditions, allowing us the construction of atomistic monolayer models.

2. Experimental

2.1. General

Melting points (uncorrected): OptiMelt, MPA 100 apparatus. Infrared (IR) spectra: Bruker FTIR IFS 113v spectrometer; KBr pellets. NMR spectroscopy: Bruker Avance 400; data given as ppm; *J* values are given in Hz; spectra referenced to the residual solvent peak; the degree of substitution of C atoms was determined by the APT method. MALDI-ToF mass spectra: Bruker, Daltonics REFLEX III. N_2-laser (337 nm), pulsed ion extraction (PIE), HIMAS-detector, acceleration voltage 20 kV, matrix: DHB. CI mass spectra: Finnigan MAT, SSQ 7000 with a single-stage quadrupole system; intensities are given relative to the base peak; CI-gas: methane. Thin layer chromatography: silica gel (Kieselgel F_{254}) on Al foils (Merck). Gravity column chromatography: silica gel (Kieselgel 60, 0.063–0.200 mm, Merck).

2.2. Synthesis procedures

10-(Decylsulfanyl)decan-1-ol (1). To a solution of dec-9-en-1-ol (300 mg, 1.7 mmol) and decane-1-thiol (335 mg, 2.1 mmol) in THF (10 mL) at 0 °C, 9-BBN (0.04 mL, 2.0 mmol; 0.5 M in THF) was added and the mixture was stirred with continuous cooling. After 2 h, the reaction mixture was allowed to warm to RT and poured in saturated NH_4Cl solution (20 mL). The organic layer was separated and the aqueous phase was extracted three times with ethyl acetate. The combined organic layers were washed three times with water and dried with sodium sulfate. The solvent was removed and the crude product was purified by Kugelrohr distillation under reduced pressure to yield **1** (476 mg, 14 mmol, 85%) as a colorless glassy oil, which changed to a colorless powder by scratching it from the glass wall of the receiving flask. M.p.: 53–54 °C; IR (KBr): $\tilde{\nu}$ = 3361.7, 2923.2, 2851.0, 1632.9, 1462.1, 1421.6, 1129.2, 1059.9, 1042.1, 762.2 cm^{-1}. ^1H NMR (400 MHz, $CDCl_3$): δ = 3.66 (t, 2H, CH_2OH, $^3J(H,H)$ = 6.6 Hz), 2.51 (t, 4H, CH_2SCH_2, $^3J(H,H)$ = 7.5 Hz), 1.63–1.55 (m, 6H), 1.40–1.28 (m, 26H), 0.90 (t, 3H, CH_3, $^3J(H,H)$ = 7.0 Hz) ppm. ^{13}C NMR (100 MHz, $CDCl_3$): δ = 63.0 (p), 32.8 (s), 32.2 (s), 32.2 (s), 31.9 (s), 29.7 (s), 29.7 (s), 29.5 (s), 29.5 (s), 29.4 (s), 29.3 (s), 29.3 (s), 29.2 (s), 29.2 (s), 28.9 (s), 28.9 (s), 25.7 (s), 22.7 (s), 14.1 (p) ppm. Signal of one secondary carbon atom is superimposed by others. MS (CI): *m/z* (%) = 359 $[M+CH_2CH_3]^+$ (16), 331 $[M+H]^+$ (100), 313 $[(M+H)-H_2O]^+$ (7). Elemental analysis calc (%) for $C_{20}H_{42}OS$: C 72.66, H 12.80; found: C 72.53, H 12.75.

4b,8b,12b-Tris(10-(decylsulfanyl)decyloxy))-12d-methyl-4b,8b,12b, 12d-tetra-hydrodibenzo[2,3:4,5]pentaleno[1,6-*ab*]inden (3). 4b,8b,12b-Tribromo-12d-methyl-4b,8b,12b,12d-tetrahydrodibenzo[2,3:4,5]pentaleno[1,6-*ab*]inden [16] **2** (50 mg, 941 μmol) was added at 70 °C to a melt of 10-(decylsulfanyl)decan-1-ol **1** (450 mg, 13.6 mmol) and subsequently the reaction mixture was vigorously stirred under argon for 12 h. Then the reaction mixture was allowed to cool to RT and the resulting residue was purified by column chromatography (chloroform) to yield **3** (96 mg, 753 μmol, 80%) as a colorless and highly viscous liquid. IR (KBr): $\tilde{\nu}$ = 3436.4, 3068.2, 3029.6, 2923.9, 2851.5, 1464.5, 1375.9, 1236.2, 1096.8, 1073.9, 767.6, 722.9 cm^{-1}. ^1H NMR (400 MHz, $CDCl_3$): δ = 7.53 ($AA'BB'_{ortho}$, 6H), 7.29 ($AA'BB'_{meta}$, 6H), 3.37 (t, 6H, CH_2OH, $^3J(H,H)$ = 7.1 Hz), 2.51 (t, 12H, CH_2SCH_2, $^3J(H,H)$ = 7.6 Hz), 1.69–1.55 (m, 21H, $-OCH_2CH_2$, $CH_2CH_2SCH_2CH_2$ and $CH_{3methyl}$), 1.40–1.29 (m, 78H, the remaining 39 CH_2 groups), 0.90 (t, 9H, ω-CH_3, $^3J(H,H)$ = 6.8 Hz). ^{13}C NMR (100 MHz, $CDCl_3$): δ = 143.3 (q), 129.1 (t), 124.5 (t), 95.9 (q), 77.9 (q), 66.6 (s), 32.2 (s), 31.8 (s), 30.6 (s), 29.7 (s), 29.6 (s), 29.5 (s), 29.5 (s), 29.5 (s), 29.4 (s), 29.3 (s), 29.2 (s), 28.9 (s), 26.1 (s), 22.6 (s), 14.1 (p), 11.5 (p). Signals of four secondary carbon atoms are superimposed by others. MS (MALDI-ToF): *m/z* calc. for ($C_{83}H_{138}O_3S_3$): 1279; found: 1302 $[M+Na]^+$, 950 $[M-C_{10}H_{21}S(C_{10}H_{20})O^\bullet]^+$, 621 $[M-C_{10}H_{21}S(C_{10}H_{20})O^\bullet-C_{10}H_{21}S(C_{10}H_{20})O^\bullet]^+$. Elemental analysis calc (%) for $C_{83}H_{138}O_3S_3$: C 77.87, H 10.87; found: C = 77.81, H = 10.78.

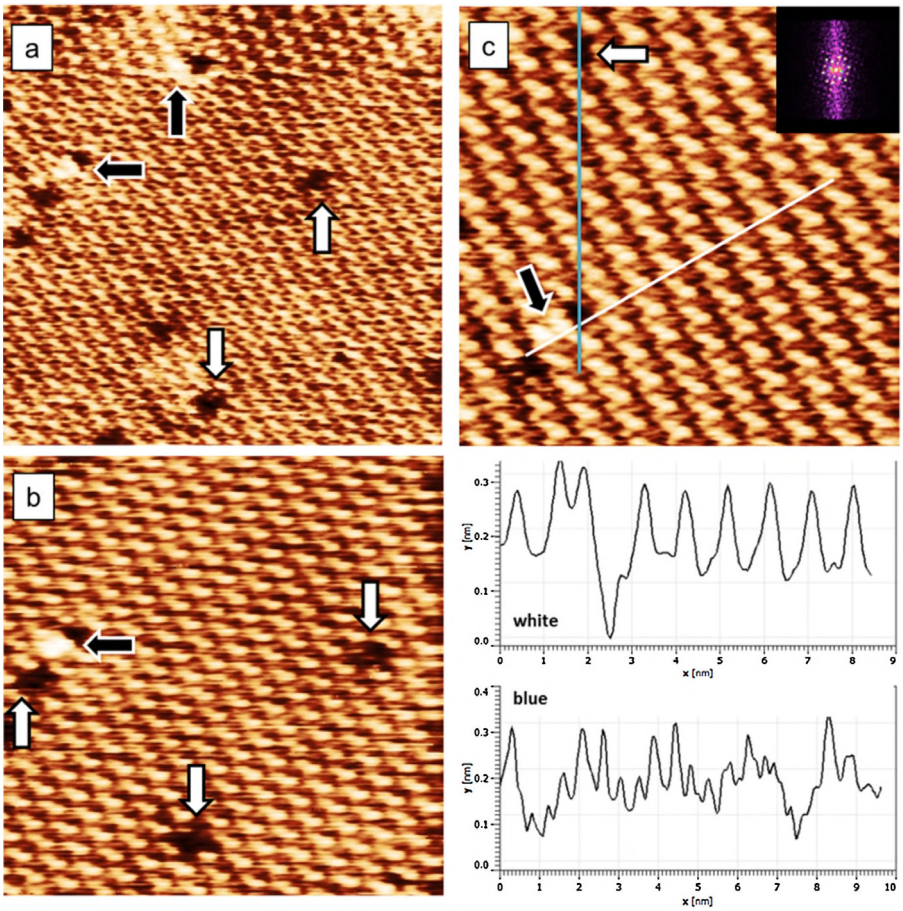

Fig. 1. STM images of mixed SAMs composed of C6-SH and **3** (stock solution: thiol: 1 mM, **3**: 0.01 mM). (a) 20 × 20, (b) 16 × 16 and (c, top) 12 × 12 nm^2 (V_t = −1.4 V, I_t = 8 pA). The close packing of C6-SH is consistent with a (2√3 × 3)R30° lattice. On all images, individual molecules of **3** appear as big bright features (black arrow), while defects of the same size appear dark (white arrow). (c, bottom) Section along the white line; inset: FT pattern of the image.

2.3. Sample preparation

Mixed SAM preparation. Commercially available gold surfaces (Arrandee™; Au films on a borosilicate glass substrate with a 2.5 nm Cr binding layer (11 × 11 mm, 250 ± 50 nm)) [17] were treated by a standard procedure before usage. Stock solutions of the thiols (1 mM in ethanol/chloroform (1:1)) and TBTQ **3** (0.01 mM in ethanol/chloroform (1:1)) were prepared in volumetric flasks that were cleaned by soaking 0.5 h in "cleaning" solution (2:1:1 $H_2O/NH_3/H_2O_2$). The vessels were thoroughly rinsed with deionized water, absolute ethanol and dried before use. The freshly tempered gold surfaces were immersed in a 1:1 mixture of the stock solutions of the adsorbates for 2 h at 50 °C. The resultant mixed SAMs were allowed to cool slowly to room temperature exhaustively rinsed with ethanol/chloroform (1:1) and dried under a flow of argon gas. STM measurements were performed with an Agilent 5500 AFM/SPM microscope with mechanically cut Pt–Ir (80:20) tips. All images were obtained under ambient conditions in constant-current mode.

3. Results and discussion

10-(Decylsulfanyl)decan-1-ol **1** was synthesized by the base-catalysed addition of decane-1-thiol and dec-9-en-1-ol (Scheme 1, a). 4b,8b,12b-Tribromotribenzotriquinacene **2** was synthesized in 6 steps according to literature procedures starting from dimethyl phthalate with an overall yield of 19% [3a,b,16]. TBTQ **3** was synthesized through subsequent substitution of the bromine atoms of 4b,8b,12b-tribromotribenzotriquinacene **2** with thioether **1** (Scheme 1, b). To ensure the three-fold S_N1-type substitution reaction in high yield (80%) thioether **1** was used in large excess, i.e. as solvent.

Similar to reactant **2**, TBTQ **3** is C_{3v} symmetrical and therefore the ^{1}H NMR spectrum shows only relatively few signals (Fig. S4). The 12 aromatic protons correspond to an AA′BB′-system at δ = 7.53 and δ = 7.29 ppm respectively. The 126 aliphatic protons correspond to three triplets at δ = 3.37, 2.51 and 0.90 ppm and two multiplets at 1.69–1.55 as well as 1.40–1.29 ppm. The ^{13}C NMR spectrum of TBTQ **3** also reflects the C_{3v} symmetry of the compound. Of the combined number of 60 carbon atoms belonging to the three thioether groups only 16 resonance peaks from δ = 66.7–14.1 ppm can be assigned, but for the C_{3v} symmetry 20 signals are expected. Probably the signals of the carbon atoms which have the longest distance to the heteroatoms and the ω-CH_3 group overlap each other. The three signals at δ = 95.9, 77.8 and 11.5 ppm correspond to the three benzylic bridgehead carbons (4), the central carbon (5) and the carbon of the central methyl group (6). The remaining aromatic carbons relate to the three signals at δ = 143.3 (1), 129.1 (2) and 124.6 (3) ppm (Fig. S5).

In the corresponding mass spectrum (MALDI-ToF; Fig. S6) the expected molecular radical ion ($[M+H]^{\bullet+}$, calcd m/z = 1279) was not detectable and only traces of $[M+Na]^+$ (calcd m/z = 1302) could be found. Instead, the largest m/z value arises for the fragments at 950 $[M-C_{10}H_{21}S(C_{10}H_{20})O^{\bullet}]^+$ and 621 $[M-C_{10}H_{21}S(C_{10}H_{20})O^{\bullet}-C_{10}H_{21}S(C_{10}H_{20})O^{\bullet}]^+$ formed by α-cleavage due to the enhanced reactivity of the

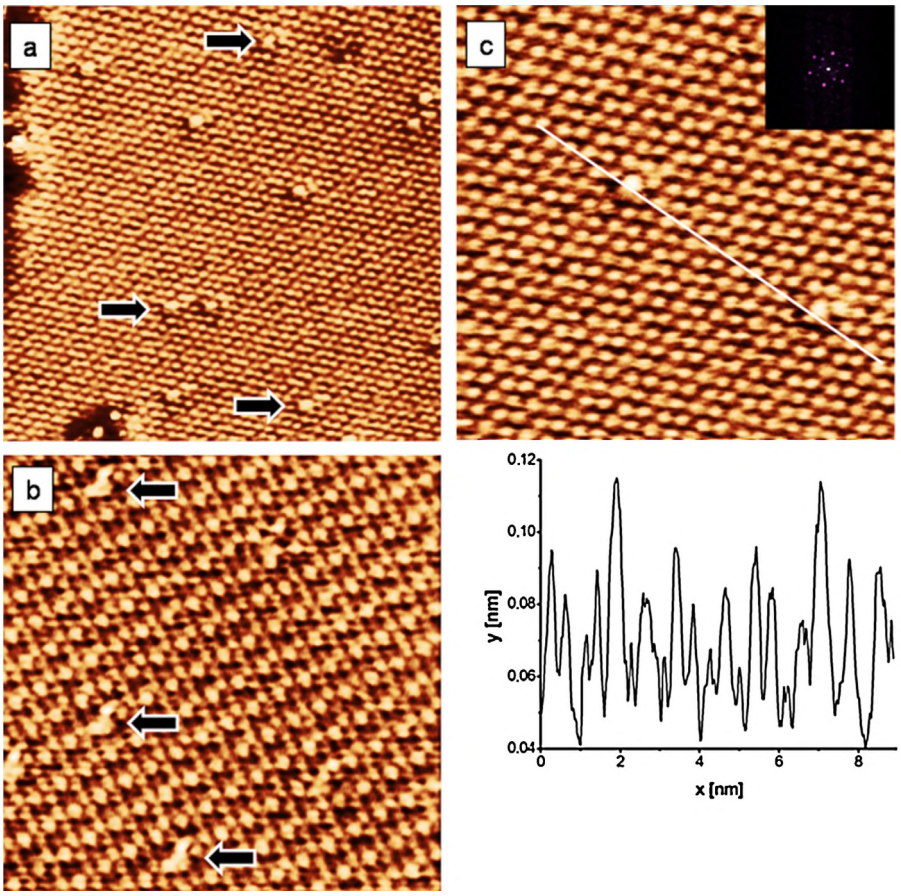

Fig. 2. STM images of mixed SAMs composed of C10-SH and **3** (stock solution: thiol: 1 mM, **3**: 0.01 mM). (a) 18 × 18, (b) 12 × 12 and (c, top) 10 × 10 nm^2 (V_t = −700 mV, I_t = 6 pA). The close packing of C10-SH is consistent with a ($\sqrt{3} \times \sqrt{3}$)R30° hexagonal lattice (for (b) ($2\sqrt{3} \times 3$)R30°). On all images, individual molecules of **3** appear as big bright features (black arrow). (c, bottom) Section along the white line; inset: FT pattern of the image.

bridgehead ether functions. This observation is in agreement with similar findings by Kuck et al. [3b] concerning bridgehead ether-functionalized 12d-methyl-4b,8b,12b,12d-tetrahydrodibenzo[2,3:4,5]pentaleno[1,6-*ab*]indenes.

Initial endeavors to form mixed monolayers between alkanethiols and TBTQ 3 were based on hexanethiol (C6-SH) assuming that TBTQ 3 would to penetrate a short-chain alkanethiol quickly and efficiently. For the anchor groups of TBTQ 3, instead of the more common thiol groups, dialkylsulfides are employed, because the sulfur atom of the latter interacts with the surface atoms of a gold layer through a relatively weak dative bond [18], which in turn should lead to faster and reversible assembly dynamics.

A study by Lavrich et al. [19] has shown that dialkylsulfides merely bind via physisorption to an Au surface and the excess physisorption enthalpy contributed by the sulfur–Au atom interactions alone is by the order of 24 kJ/mol when compared to the physisorption enthalpy shown by a structurally related *n*-alkane. In contrast to dialkyldisulfides, alkanethiols show a chemisorption enthalpy of 126 kJ/mol, which is independent of chain length. However, since it is the difference in Free Gibbs energy values which determines the ratio between the surface-bound species in a mixed SAM, the influences of solvent effects, time, temperature etc. are not well covered by comparing binding enthalpies alone.

Experimentally we have observed, in agreement with other studies [12–14] that during the dynamic process of SAM formation intermolecular van der Waals interactions are important driving forces for the formation of the mixed monolayer. Moreover, the number of three dative bonds between the dialkylsulfide chains of TBTQ 3 and the Au surface in conjunction with the much higher dispersive interactions of the dialkylsulfide tails seems to overcompensate the much stronger Au–S bonding interaction of the alkanethiols.

Intending to improve the structural order of the mixed adsorbates on gold, the formation of the mixed SAM was performed at relatively high temperature, i.e. 50 °C [20,21].

In Fig. 1, STM images of a mixed SAM consisting of C6-SH and TBTQ **3** are shown.

C6-SH forms a rectangular primitive unit mesh of the characteristic ($2\sqrt{3} \times 3$)R30° lattice structure, where $2\sqrt{3}$ and 3 are the multiplicative factors of the Au-(1 1 1) lattice constant *a* (*a* = 0.288 nm) [22], and indicates the Au–Au inter atomic distance on the Au-(1 1 1) surface [23]. The measured cell dimensions of 0.99 × 0.84 nm^2 are very close to the theoretically expected values of 1.00 × 0.86 nm^2. We assume from the literature (Ref. [24]) that the alkyl chains are tilted in a uniform direction, adapting a 30° angle with respect to the surface normal of the Au-surface. The variation in height of the monolayer is based upon different conformations. The threefold hollow site of the Au-(1 1 1) lattice was assigned as the preferred adsorption site [24c] and we used the observation of this reference to create the model in Fig. 3.

All images show several bright features of the same shape and size with a diameter of 0.85 ± 0.05 nm. This leads us to the assumption that individual molecules of **3** are embedded in the monolayer of (C6-SH). However, even more frequently we observe analogous black features representing defects in the C6-SH surface lattice. These vacancies, formerly occupied by individual molecules of **3**, are supposed to originate from excessive cleaning of the resulting surface prior to STM measurement.

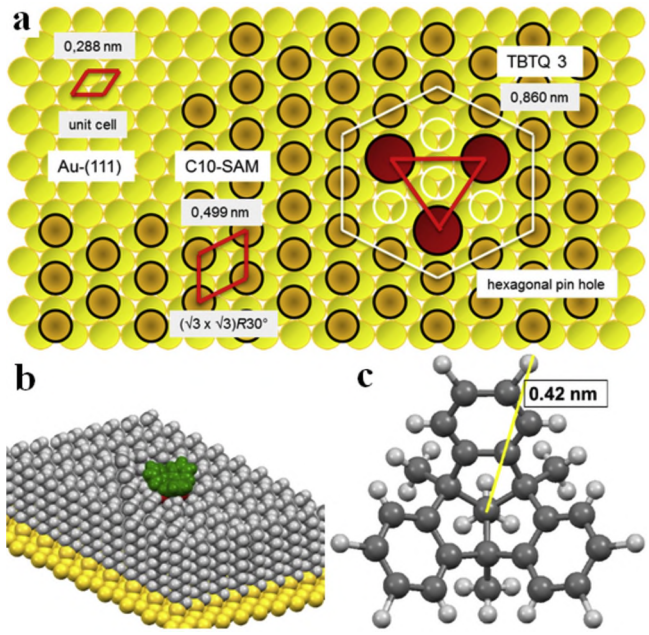

Fig. 3. Schematic representation in top view (a) of the highly ordered mixed SAM consisting of C10-SH and TBTQ **3**, substituting a hexagonal pin hole on Au-(1 1 1); associated structural model (UFF force field, (b); TBTQ unit in top view (c) and its radius, calculated from the single crystal data collected from two TBTQ derivatives (see Refs. [5,7]).

Because of that and the fact that the assembly dynamics of long-chain alkanethiols are known to be faster than those of short-chain alkanethiols [25] we repeated investigations on formation of mixed SAM, employing this time decanethiol (C10-SH) as the main monolayer component in order to enhance the intermolecular interaction between alkanethiol and **3**.

In Fig. 2, STM images of a mixed SAM consisting of C10-SH and **3** are shown. There is a clear distinction between the components attributed to different shapes and lateral sizes. Apart from the already described $(2\sqrt{3}\times 3)$R30° lattice structure for C6-SH (Fig. 1), the typical hexagonal lattice structure for alkanethiols can be observed. This surface is described as a $(\sqrt{3}\times\sqrt{3})$R30° structure, where $\sqrt{3}$ is the multiplicative factor of the Au-(1 1 1) lattice constant *a* [26]. The measured cell dimensions of $0.48\times 0.48\,nm^2$ are very close to the theoretically expected values of $0.50\times 0.50\,nm^2$. Like for the C6-SH-layer, the alkyl chains are tilted by a 30° angle away from the normal of the Au-surface.

As in the previous case, no formation of separate domains of TBTQ **3** and C10-SH can be observed on the Au-(1 1 1) surface. Individual molecules of **3** are incorporated into the C10-SH SAM and appear as protrusions with uniform shape in each case. In contrast to the C6-SH-**3** mixed layer no vacancies can be observed. A closer look at Fig. 2c provides several interesting properties of the mixed monolayer. The constant current height difference between **3** and C10-SH is only between 20–25 pm, in contrast to 40–60 pm in the case of the C6-SH-layer, and likely leads to the extraordinary resolution of the measurement. This similarity in the apparent height is related to the current transport properties, reflecting – beside the physical height – the similar transconductance of the layer-forming molecules [27]. The lateral extension of **3** is 0.85 ± 0.05 nm (real size = ca. 0.84 nm, Fig. 3c).

The absence of defects in the environment as well as the uniform shape and dimension of the minor component suggest that individual molecules of **3** are embedded in the highly ordered C10-SH-SAM, tilted in a 30° angle from the surface normal. Because di-*n*-decyl sulfide chains require almost twice the space of C10-SH, TBTQ **3** aligns within a hexagonal pin hole, whereas the sulfide atoms bind to the threefold hollow sites of a 0.86 nm equilateral triangle (Fig. 3a). The arrangement induces four adsorption defects, three on the corner and one in the center of the hexagon. This leads to a densely packed alkyl chain layer underneath the TBTQ head group, which accordingly is exposed to the top of the surface layer (Fig. 3b).

4. Conclusions

In this work, we have presented the synthesis of TBTQ **3**, a novel tribenzotriquinacene derivative with backbone-attached thioether groups. Single molecules of **3** were successfully embedded in a mixed SAM comprising single chain alkanethiols (C6-SH, C10-SH) as major component. The preparation procedure and the characterization of the SAMs were performed under ambient conditions.

While the usage of C6-SH as matrix was leading to monolayer stability issues – most TBTQ molecules were removed from the mixed SAM during the cleaning procedure – a mixed monolayer with highly ordered domains of C10-SH containing individually dispersed molecules of TBTQ **3** was prepared. The STM investigations prove that **3** becomes fully embedded into the alkanethiol matrix, leading to a densely packed alkyl chain layer underneath the surface-exposed TBTQ headgroup. The alternative option, the formation of loose adsorbates of **3** residing on top of (structurally perfect) alkanethiol monolayer can thus be safely ruled out.

In summary, we present a versatile method for the deposition of TBTQ-based components on flat Au-(1 1 1) surfaces. Owing to their structural properties and functional features, TBTQ components are considered attractive candidates for future surface-anchored nanodevices that self-assemble from suitably designed molecular building blocks.

Acknowledgement

The authors are grateful to the German Science Foundation for financial support (DFG grant VO829/6-1).

Appendix A. Supplementary data

Supplementary data associated with this article can be found, in the online version, at http://dx.doi.org/10.1016/j.apsusc.2015.08.106.

References

[1] (a) K. Mislow, Chemtracts Org. Chem. 2 (1989) 151–174;
(b) J.F. Stoddart, V. Balzani, A. Credi, F.M. Raymo, Angew. Chem. Int. Ed. 39 (2000) 3348–3391;
(c) T.R. Kelly (Ed.), Molecular machines, Top. Curr. Chem. 262 (2005) (special volume);
(d) W.R. Browne, B.L. Feringa, Nature Nanotechnol. 1 (2006) 25–35;
(e) M.M. Pollard, M. Lubomska, P. Rudolf, B.L. Feringa, Angew. Chem. Int. Ed. 46 (2007) 1278–1280.
[2] (a) A. Globus, C.W. Bauschlicher Jr., J. Han, R.L. Jaffe, C. Levit, D. Srivastava, Nanotechnology 9 (1998) 192–199;
(b) Y. Shirai, A.J. Osgood, Y. Zhao, K.F. Kelly, J.M. Tour, Nano Lett. 5 (2005) 2330–2334;
(c) J.-F. Morin, Y. Shirai, J.M. Tour, Org. Lett. 8 (2006) 1713–1716.
[3] (a) W.A. Moser, R.W. Soeder, J. Org. Chem. 36 (1971) 1561–1563;
(b) D. Kuck, A. Schuster, R.A. Krause, J. Tellenbröker, C.P. Exner, M. Penk, H. Bögge, A. Müller, Tetrahedron 57 (2001) 3587–3613;
(c) D. Kuck, Chem. Rev. 106 (2006) 4885–4925;
(d) J.G. Brandenburg, S. Grimme, P.G. Jones, G. Markopoulos, H. Hopf, M.K. Cyranski, D. Kuck, Chem. Eur. J. 19 (2013) 9930–9938.
[4] (a) P.E. Georghiou, L.N. Dawe, H.-A. Tran, J. Strübe, B. Neumann, H.-G. Stammler, D. Kuck, J. Org. Chem. 73 (2008) 9040–9047;
(b) T. Wang, Z.Y. Li, A.L. Xie, X.J. Yao, X.P. Cao, D. Kuck, J. Org. Chem. 76 (2011) 3231–3238.
[5] B. Bredenkötter, S. Henne, D. Volkmer, Chem. Eur. J. 13 (2007) 9931–9938.
[6] (a) S. Henne, B. Bredenkötter, A.A.D. Baghi, R. Schmid, D. Volkmer, Dalton Trans. 41 (2012) 5995–6002;

(b) S. Henne, B. Bredenkötter, M. Alaghemandi, S. Bureekaew, R. Schmid, D. Volkmer, Chem. Phys. Chem. 15 (2014) 3855–3863.
[7] B. Bredenkötter, M. Grzywa, M. Alaghemandi, R. Schmid, W. Herrebout, P. Bultinck, D. Volkmer, Chem. Eur. J. 20 (2014) 9100–9110.
[8] (a) H.E. Katz, G. Scheller, T.J. Putvinski, M.L. Schilling, W.L. Wilson, C.E.D. Chidsey, Science 254 (1991) 1485–1487;
(b) A.K. Kakkar, S. Yitzchaik, S.B. Roscoe, F. Kubota, D.S. Allan, T.J. Marks, W. Lin, G.K. Wong, Langmuir 9 (1993) 388–390.
[9] (a) L.H. Dubois, R.G. Nuzzo, Annu. Rev. Phys. Chem. 43 (1992) 437–463;
(b) J.B. Schlenoff, M. Li, H. Ly, J. Am. Chem. Soc. 117 (1995) 12528–12536.
[10] (a) R.G. Nuzzo, F.A. Fusco, D.L. Allara, J. Am. Chem. Soc. 109 (1987) 2358–2368;
(b) H. Keller, W. Schrepp, H. Fuchs, Thin Solid Films 210/211 (1992) 799–802.
[11] (a) E.B. Troughton, C.D. Bain, G.M. Whithesides, D.L. Allara, M.D. Porter, Langmuir 4 (1988) 365–385;
(b) E. Katz, N. Itzhak, I. Willner, J. Electroanal. Chem. 336 (1992) 357–362.
[12] (a) C.-J. Zhong, M.D. Porter, J. Am. Chem. Soc. 116 (1994) 11616–211617;
(b) B.H. Huisman, E.U.T. van Velzen, F.C.J.M. van Veggel, J.F.J. Engbersen, D.N. Reinhoudt, Tetrahedron Lett. 36 (1995) 3273–3276;
(c) B.T. Houseman, M. Mrksich, Angew. Chem. Int. Ed. Engl. 38 (1999) 782–785.
[13] (a) E.U.T. van Velzen, J.F.J. Engbersen, D.N. Reinhoudt, J. Am. Chem. Soc. 116 (1994) 3597–3598;
(b) U. Eggo, T. van Velzen, J.F.J. Engbersen, P.J. de Lange, J.W.G. Mahy, D.N. Reinhoudt, J. Am. Chem. Soc. 117 (1995) 6853–6862.
[14] S. Zhang, A. Palkar, A. Fragoso, P. Prados, J. de Mendoza, L. Echegoyen, Chem. Matter. 17 (2005) 2063–2068.
[15] (a) C.E.D. Chidsey, R.W. Murray, Science 231 (1986) 25–31;
(b) M.T. Cygan, T.D. Dunbar, J.J. Arnold, L.A. Bumm, N.F. Shedlock, T.P. Burgin, L. Jones, D.L. Allara, J.M. Tour, P.S. Weiss, J. Am. Chem. Soc. 120 (1998) 2721–2732;
(c) N. Battaglini, H. Klein, P. Dumas, C. Moustrou, A. Samat, Appl. Surf. Sci. 212–213 (2003) 481–484.
[16] D. Kuck, A. Schuster, B. Paisdor, D. Gestmann, J. Chem. Soc., Perkin Trans. 1 (1995) 721–732.
[17] http://arrandee.com/usage.html
[18] H. Schoenherr, G.J. Vancso, B.-H. Huisman, F.C.J.M. Van Veggel, D.N. Reinhoudt, Langmuir 15 (1999) 5541–5546.
[19] D. Lavrich, S. Wetterer, S. Bernasek, G. Scoles, J. Phys. Chem. B 102 (1998) 3456–3465.
[20] H. Takiguchi, K. Sato, T. Ishia, K. Abe, K. Yase, K. Tamada, Langmuir 16 (2000) 1703–1710.
[21] R. Yamada, H. Wano, K. Uosaki, Langmuir 16 (2000) 5523–5525.
[22] P. Villars, L.D. Calvert, Pearson's Handbook of Crystallographic Data for Intermetallic Phases, 2nd ed, ASM International, USA, 1991.
[23] G.E. Poirier, M.J. Tarlov, Langmuir 10 (1994) 2853–2856.
[24] (a) L.H. Dubois, R.G. Nuzzo, Annu. Rev. Phys. Chem. 43 (1992) 437–463;
(b) G.E. Poirier, Chem. Rev. 97 (1997) 1117–1128;
(c) L.H. Dubois, B.R. Zegarski, R.G. Nuzzo, J. Chem. Phys. 98 (1993) 678–688.
[25] C.D. Bain, H.A. Biebuyck, G.M. Whitesides, Langmuir 5 (1989) 723–727.
[26] C.A. Widrig, C. Alves, M.D. Porter, J. Am. Chem. Soc. 113 (1991) 2805–2810.
[27] M. Bowker, P.R. Davies (Eds.), Scanning Tunneling Microscopy in Surface Science, Nanoscience and Catalysis, Wiley-VCH Verlag GmbH & Co KGaA, Weinheim, 2010, ISBN 978-3-527-31982-4, Chapter 4.